

A Review Article on Fatigue Life Estimation of Miter Bend

Nirav Rathod^{1*} and Dilip Patel²

¹Research Scholar, Research Scholar Gujarat Technological University, Ahmedabad - 382424, Gujarat, India; nbr.fetr@gmail.com

²GIDC Degree Engineering College, Mechanical Engineering Department, Navsari – 396406, Gujarat, India; pateldcp@gmail.com

Abstract

The Efficiency of the piping system largely relies upon bends used to connect pipes. The piping system is at the highest risk due to stress concentrations at abrupt cross-sectional change, large support less valves, vibrations, and lack of the assessment of fatigue failure. Bends undergo different combine loads involving internal pressure, in plane cyclic loading, out of plane cyclic loading, dead weight along with different thermal conditions. Compared to straight pipe miter bend has more complex mechanical behavior and critical stress-strain locations due to its asymmetric shape and hence miter bend undergoes plastic failure in the form of collapse, ratcheting, and fatigue that leads to component failure at the end. This paper presents review for behavior of miter bend considering important fracture mechanics parameters such as limit and collapse load, local wall thinning, ratcheting, creep, and their effects on fatigue life. The review also tabulates all fatigue life equations used by researchers for predicting fatigue life. Topics for further research on miter bends such as out of plane loading, vibration induced fatigue and creep are also noted.

Keywords: Fatigue Life Estimation, Miter Bend, Ratcheting

1.0 Introduction

Flow control in pipelines during material transport is the prime concern in the mining industry. For the transport of abrasive materials, slurries, or bulk solids, the Miter bends (i.e., miter elbows) might be the most useful as it is designed to change the direction of the flow of material around the corner with minimum available space. During the mining, the environment is harsh. Miter bend provides wear resistance, while constructed from hardened steel. Additional durability can be provided with ceramic lining. Miter bends offers minimize pressure drop. Hence, pumping and conveying could be operated efficiently to achieve optimum flow rate. Material flows smoother

while conveying during mining. It reduces the blockages and clogs in the pipeline while conveying coarse abrasive materials. Specific angles can be manufactured to produce Miter bend according to the layout of mining facilities and space constraints. It elevates the efficiency of the material handling system. Maintenance is considerably low due to fewer replacements, downtime, and operational costs. Miter bend can be customized according to specific requirements such as material composition, pressure, and temperature to fulfill the specific challenges that occur during the mining operation. So, it is suggested that by proper design, installation, material selection, and maintenance Miter bend can improve the performance of the conveying operation within the mining industry.

*Author for correspondence

Miter bends are extensively used in industries for large diameter pipe work mainly in nuclear power plants, chemical industries, Sewage treatment plants and desalination plants where use of round bends is either uneconomical or impractical. Miter bends provides manufacturing feasibility while dealing with large diameter and non-standard sizes piping work. In general, Miter bends are midway solution as it optimizes functional requirement and cost. Most importantly, Miter bends are broadly used in pebble bed and fusion reactors. However, various piping codes are not thoroughly covering miter bend design for different applications and for various combine loadings.

However, there are wide research scopes to know the margin of safety especially when bends are prone to failure. In addition, behaviour of the miter bend when exposed to different loading is not apparent and inadequately depicted in piping standards. As several researchers have investigated behaviour of miter bends in last decade and still there are so many areas where attention is required. Fatigue failure, shakedown regimes, and limiting load are widely studied by researchers to access the loading capacity and failure behaviour of miter bend. Therefore, in reference to studies published previously, this article reviews important influencing parameter that yields fatigue failure of miter bend.

2.0 Loading Conditions of Miter Bends

Miter elbow is fabricated by oblique cutting of metal

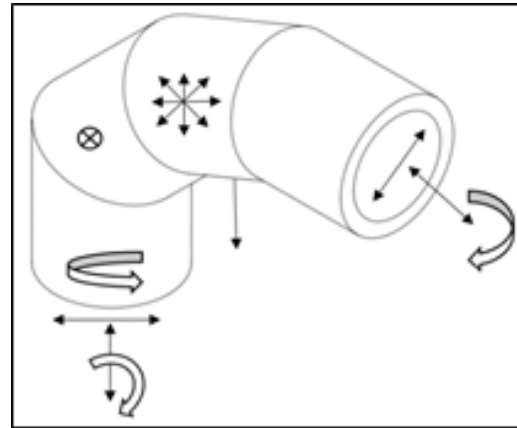


Figure 1. Miter Bend subjected to combine loads.

pipes. Cut metal pipes are welded together to form a miter bend. One weld (1W) 90° miter bend is made by cutting pipe at 45° and two weld (2W) 90° miter bend is prepared by cutting three pipe pieces at 22.5°. Similarly, different miter configuration is made by calculating miter offset and angle of cut as per requirement.

Pipe bends are subjected to combination of loads such as cyclic In Plane Bending (IPB), Out of Plane Bending (OPB), Internal Pressure (PRESS), Torsion (TORS) and environment effect and thus their behavior changes along with the active combine loads. Apart from that, piping vibration is also induced mainly due to acoustic (variation in fluid pressure with varying time), momentum (variation in fluid density and fluctuation in fluid velocity with varying time) and machinery (unbalanced forces induced from improper foundation of machinery) that

Load Sign			
Internal Pressure (PRESS)		Dead Weight	
In Plane Bending (IPB)		Torsion (TORS)	
Out of Plane Bending (OPB)		Shear Force	
Normal Force		Temperature (Environment/Medium Temperature)	

Figure 2. Load signs of miter bend.

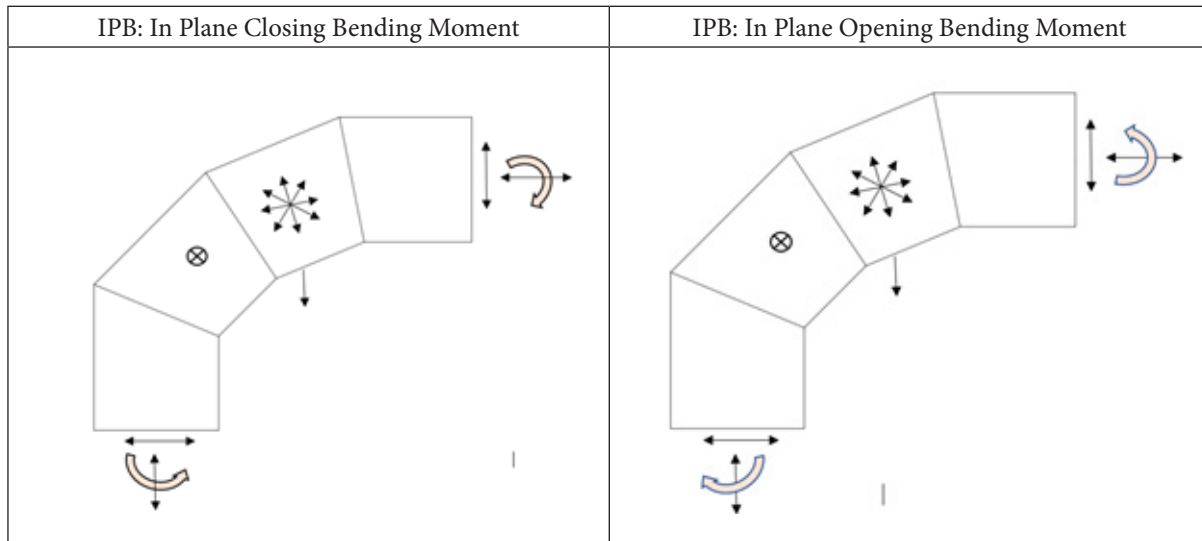


Figure 3. In plane opening and closing bending moment.

cause fatigue failure of the component. Figure 1 and Figure 2 shows combine loads acting on miter bend and load signs of miter bend respectively.

Further, in plane bending leads to either in plane opening of the miter bend or in plane closing of the miter bend depending upon the load directions on the bend as shown in Figure 3.

Pressure components are frequently subjected to cyclic loading that induces stresses at critical regions, and this requires careful attention on permissible value of yielding to analyze behavior of component. The following load situations could lead to component failure when exposed to cyclic loads.

- Elastic Deformation: Component may fail due to High Cycle Fatigue (HCF) i.e. small magnitude of maximum load and maximum number of cycles.
- Plastic Deformation: Plastic collapse of component when maximum load is greater than yield limit
- Incremental plastic collapse: Maximum load is between yield limit and plastic collapse limit that leads to either accumulation of plastic strain (Ratcheting) or shakedown.

3.0 Stress Analysis of Miter Bend

Numerous researchers have carried out investigations to understand the mechanical behaviour for analysing the

reliability of bends that are subjected to cyclic IPB, OPB, PRESS, TORS and environment effect. Stress analysis was performed by many researchers by considering various loading condition for the structural assessment of miter bend.

Elastic stress analysis of two straight circular cylindrical bend which are welded together over a plane section was conducted by Green and Emmersion¹. Using the 3-dimensional elasticity theory, general theoretical solution of axial stress and hoop stress of miter bend were derived. Stresses were evaluated at the bend under internal pressure and pure symmetrical couple. However later study proved that the solution of axial stress for bending load was not in good agreement with other research. Derived general equation of hoop and axial stress were established as base for further research studies.

Street developed theory for predicting stress distribution of multi miter and single miter bend subjected to PRESS. Medium and short length segments of bend were validated with experiment and were found in good agreement².

Bond³ carried out theoretical analysis to develop stress distribution and flexibility factor related to out of plane bending for three-weld right angled multi-miterd pipe bends. Maximum stress ratio and flexibility factor was calculated in longitudinal and circumferential direction for different pipe bend parameters. It is observed that stress

values of edge segment correction were insignificant if angle between normal section of pipe and oblique section of pipe is smaller (usually less than) and so investigation could yield precise bend predictions.

Stress analysis of miter elbows with complex configuration subjected to general loading condition was accomplished by Watanabe and Ohtsubo⁴. Ring element was proposed for stress analysis and shape functions were derived by trigonometric equations and Hermitian polynomials of second order in longitudinal and circumferential directions respectively. Observations have shown that developed FEM required less degree of freedom than the conventional shell element for the same accuracy. Moreover, it was observed that stress at the junction was higher by 20% for out of plane bending and in plane bending compared to ASME code. Stress concentration at junctions was accurately investigated as displacement components were defined in the incline cross sections of the miter bend.

Strain distribution of right-angled composite glass reinforced multi miter pipe elbow was investigated by Kitching and Hose⁵ for out of plane bending, internal

pressure and in plane bending being applied separately. Strain ratios were computed for all three types of loading by FEA, and it has been noted that discontinuities at the miter edge of inside PVC lining caused higher strain ratio distributions. Furthermore, for low miter angle (11.25°) theory of smooth pipe bend was found appropriate in external bending conditions. For pressure load, strain distribution ratio was identical in the region of intrados of smooth bend with that of miter bend in extrados region.

Wood⁶ has documented structural behaviour of various miter bends including the effects of combinations of loading and also reviewed effect for different structural parameters like out of circularity, leg length and thickness.

Elastic stress examination of miter joint used in pipeline subjected to in plane bending and internal pressure was carried out by Zhou *et al.*⁷. Based on expressions given by Green¹, the closed form theoretical results of axial and hoop stresses were attained as functions of the half miter angle, circumferential angle and radial location. Results indicated that maximum tensile stress located at outside

Table 1. Comparison of stress concentration factor for miter bends under internal pressure.

Configurations	1M	2M	3M
No. of Weld	1-weld	2-weld	3-weld
Radius (m)	0.0508	0.1572	0.1572
Thickness (mm)	5.0800	9.1440	9.5250
Bend Radius	0.2500	0.4572	0.4572
Tangent Pipe	0.1056	0.2500	0.2500
Miter Angle			
Material	Araldite	Steel	Steel
Young's Modulus	3.0	19.5	19.5
Poison's Ratio	0.49	0.30	0.30
	Stress Concentration Factor (SCF)		
Experimental	2.5	1.9	1.5
Bond and Kitching ³ , Theoretical	2.3	2.2	1.9
Chang ⁸ , FEA	2.5	2.0	1.4

surface of intrados and stresses increased with increase in miter angle.

Chang and Redekop⁸ carried out a linear stress analysis of pressurized 1 weld (1M), 2 welds (2M), 3 weld miter (3M) mitered pipe bends using finite element method based on shell element to determine stress concentration factor. It has been observed that 3 weld mite bend is subjected to minimum stress concentration and 1M bend is subjected to maximum stress concentration than 2M and 3M. Furthermore, it is to be noted that apart from configuration of miter bend, magnitude of stress concentration factor changes with change in cross sectional radius, shell wall thickness and tangent pipe length. Results indicated need of flange or stiffening ring as reinforcement in joint regions affected by cross-sectional flattening. Bond and Kitching³ and Chang⁸ compared calculated stress concentration factor as shown in Table 1.

Local behaviour of stress near to oblique weld of single miter bend was investigated by Orynyak⁹ under bending moment and internal pressure with the application of short and long cylindrical shell solutions. Solutions obtained from the developed mathematical model gave the possibility to solve the shell problem by using two equations of fourth order instead of equation of eighth order as results obtained were in good agreement with numerical study.

Colquhoun¹⁰ analysed hoop stress distribution of miter bend ranging from 1 to 5 degree and diameter to thickness ratio of 60 and 80. Temperature differential iterations (goal seek) were used to determine what temperature difference would yield a combined von mises stress of 100% specified minimal yield strength.

More recently DUBYK *et al.*¹¹ assessed stresses of single miter bend using long and short solutions of shell theory. Investigation was conducted to substitute equation of eighth order of shell theory by long and short solutions of shell theory. Main variables associated with short solutions such as angle, moment, lateral force and radial displacement and main variables of long solutions such as axial force, axial displacement, circumferential displacement, and lateral force were derived. Hence explicit equations for all the main variables were derived and that can be used to develop FEA models for the future research. It was found that for simple case when miter bend is subjected to only internal pressure short solution

is preferable whereas for a more complex case of bending moment both short and long solution is preferable as it is fairly consistent with the experimental and numerical data.

4.0 Fracture Mechanics and Fatigue

Most of the piping components are failed due to fatigue loading and as a result failure may occur well below allowable stress limit. This failure may occur due to the presence of flaws which was either undetected during pre-inspection or generated during service.

4.1 Plastic Collapse and Limit Load

Over the years many researchers have examined plastic load and limit load of various miter configuration subjected to different loadings. Table 2 thoroughly summarises the collapse load and gross load of the various miter bends subjected to different geometrical dimensions, material and loading conditions. Data summarised in Table 2 are based on experiments conducted by various researchers over the years and it was later quoted by Wood⁶ and Neilson *et al.*¹² as shown by serial number 1 to 9 and serial number 10, respectively. Results presented in the table are recorded either by conducting experiments or using finite element analysis.

4.2 Fatigue Life Estimation

Many researchers have extensively conducted numerical analysis and experimental study of pipe bends under combination of loading mainly cyclic in plane/ out of plane cyclic bending, internal pressure and seismic load. Numerical analysis was mostly simulated using FEA packages such as ANSYS and ABAQUS over the last few decades. Numerical investigation of bends helps in interpreting ratcheting behavior and thereby estimating fatigue life of pipe bends. Researchers have developed various material model such as the Chaboche non-linear kinematic models, non-linear material using incremental plasticity with the Von Mises yield function and isotropic hardening, the non-linear kinematic hardening Ohno-Wang (OW) II linear kinematical hardening etc. that helps the research enthusiast to choose appropriate constitutive model.

Table 2. Plastic load and limit load of miter bends.

S. No.	Loading	Configuration	Parameter	General/Gross load	Collapse load	(Collapse load)/(Gross load)	Remark
1	IPB	90°, 5 segments, miter	-	$F_{GY} = 6676 \text{ N}$			F_L not obtained as test was not conducted till it fails.
2	IPB PRESS	90° Double Segment 3W	a) Increasing Bend Angle b) Reducing Bend Angle c) PRESS	a) $M_{FY} = 40241 \text{ N.m}$ b) $M_{FY} = 41759 \text{ N.m}$ c) $P_{FY} = 6.9 \text{ N/mm}^2$	a) $M_L = 264475 \text{ N.m}$ b) $M_L = 194271 \text{ N.m}$ c) $P_L = 25.5 \text{ N/mm}^2$	a) $M_L/M_{FY} > 6.5$ b) $M_L/M_{FY} = 2.5$ c) $P_L/P_{FY} = 3.7$	a) Test was discontinued at 264475 N m as no failure was indicated. b) Bursting pressure recorded was 25.5 N/mm ² for the miter bend, whereas for equivalent straight pipe a burst pressure of 25.6 N/mm ² was recorded.
3	IPB PRESS	90° Single Segment 2W	a) Increasing Bend Angle b) Reducing Bend Angle c) PRESS	a) $M_{GY} = 97691 \text{ N.m}$ b) $M_{GY} = 47833 \text{ N.m}$ c) $M_{PY} = 12.4 \text{ N/mm}^2$	a) $M_L = 187284 \text{ N.m}$ b) $M_L = 95160 \text{ N.m}$ c) $P_L = 20.0 \text{ N/mm}^2$	a) $M_L/M_{GY} = 1.9$ b) $M_L/M_{GY} = 2.0$ c) $P_L/P_{FY} = 3.7$	a) *Test rig failed at maximum moment of 18,7284 N.m. b) Bursting pressure of 20 N/mm ² for the miter elbow was recorded compared to a burst pressure of 24.5 N/mm ² for equivalent straight pipe.
4	PRESS	90° reinforced steel miter	-	$P_{FY} = 2.8 \text{ N/mm}^2$ $P_{GY} = 5.4 \text{ N/mm}^2$	$P_L = 9.6 \text{ N/mm}^2$	$P_L/P_{FY} = 3.5$ $P_L/P_{GY} = 1.8$	An elliptical insert-cascade band was used for reinforcement
5	IPB	90° single un-reinforced aluminium miter bend	Reducing Band Angle	$F_{GY} = 1868 \text{ N}$	$F_L = 6161 \text{ N}$	$F_L/F_{GY} = 3.3$	At load above 2002 N, load-deflection relationship became time dependent. Test rig was failed while investigating a 120° bend.

6	IPB	90° Two Segment 3W	Reducing Band Angle	$F_{GY} = 2135 \text{ N}$	$F_L = 4239 \text{ N}$	$F_L/F_{GY} = 2$	
7	PRESS	Single un-reinforced steel miter	-	$P_{FY} = 1.9 \text{ N/mm}^2$ $P_{GY} = 5.5 \text{ N/mm}^2$	$P_L = 7.2 \text{ N/mm}^2$	$P_L/P_{FY} = 3.9$ $P_L/P_{GY} = 1.8$	For pressure value above 5.5 N/mm^2 gross plastic deformation was detected.
8	PRESS	90° miterd bends reinforced with elliptical inserts	-	For $a/t = 25$, 5.4 N/mm^2 For $a/t = 43$, $P_{FY} = 3.7 \text{ N/mm}^2$	For $a/t = 25$, P_L was not obtained For $a/t = 43$, $P_L = 12.5 \text{ N/mm}^2$	For $a/t = 43$, $P_L/P_{FY} = 3.37$	During elastic behaviour internal pressure increased the bend angle whereas for plastic behaviour internal pressure reduced the bend angle.
9	IPB	90° 1W Miter Bend	Load and Displacement controlled Force	$M_{FY} = 23230 \text{ N.m}$	$M_L = 33510 \text{ N.m}$	$M_L/M_{FY} = 3.9 = 1.44$	FEA solution of plastic collapse was validated by experimentation, and it was in excellent agreement with experimental results.
10	IPB	90° Single Segment	Reducing Band Angle	$F_{GY} = 16000 \text{ N}^*$	$F_L = 22890 \text{ N}$	$F_L/F_{GY} = 1.43$	* Nonlinearity of load vs deflection curve was observed at approximately 16000N

Shakedown and ratcheting domains of round 90-degree bend under fluctuating load have been at the significant attention over the past decades but such research studies are still lacking for miter bends subjected to various combined loads. However, many research studies have been conducted over the years for fatigue life estimation of various bends and improved mathematical models are developed over the years for accurate results.

Rahman *et al.*¹³ evaluated seven cyclic plasticity models for structural ratcheting response simulations of straight pipes subjected to uniform internal pressure and cyclic bending. Seven plasticity models namely Modified Chaboche (Bari and Hassan), Abdel Karim–Ohno,

Multilinear (Besseling), Ohno–Wang, bilinear (Prager), Modified Ohno–Wang (Chen and Jiao) and Chaboche were evaluated. It has been found that, for analysing the pipe with varying straight pipe diameter and for assessing circumferential strain ratcheting none of the seven-plasticity model executed satisfactorily result. Furthermore, it is observed that numerical investigation using multi linear model was best among all seven evaluated models but still it lacks in computing fatigue life and damage accumulation.

Goyal¹⁴ conducted experiment to investigate fatigue ratcheting on bends made of SS304 LN stainless steel elbows of 168 mm outer diameter and average

thickness 15 mm under action of internal pressure and pure cyclic bending. Ultrasonic Technique (UT) based thickness measuring gauge was used to measure the elbow thickness at various locations before, after and at regular intervals during the tests. It is observed that crack initiation, take place at inside surface in the crown region of elbow and it grown till it becomes through thickness crack. The number of cycles needed to start a crack was detected using UT scanning. The through-thickness crack was observed near the crown locations with axial orientation. Elbows were failed by existence of through-thickness crack along with local ballooning. The elbows experienced significant ballooning due to ratchet strain accumulation. It was found that number of cycles to crack initiation estimated by ASME mean fatigue life curve and classical low cycle fatigue assessment varies between 5500 cycles to 19000 cycles, but results indicated that even final through wall rupture occurred in 71 to 282 cycles that showed significance of local accumulation (ratcheting) of strain.

Li *et al.*¹⁵ carried out both experiment and finite element analysis of fatigue and ratcheting of miterd pipe elbows subjected to combine load of bending and internal pressure. It has been observed that failure occurred due to low cycle fatigue and crack is developed, initiated, and propagated resulting in leakage in very few cycles. Build-up of ratcheting strain caused low cycle fatigue and hence ductility was exhausted. It was found that material model used for simulating the strain hardening mechanism was not accurate enough to validate actual strain level test data from experimentations. Displacement was evaluated using Chaboche material model that results into lower displacement value as compared to experimental data and it was concluded that used material model was too stiff. Whereas Basquin-Coffin Manson equation and Modified equation were used to predict fatigue life. Basquin-Coffin Manson equation over predicted fatigue life whereas Modified equation appeared to be accurate in predicting fatigue life.

Korba *et al.*¹⁶ performed shakedown analysis on 90-degree miter pipe bends using simplified direct non-cyclic method to identify shakedown boundaries. Miter bend configurations with one weld (1W), two weld (2W) and three weld (3W) were tested and analysed under both in plane and out of plane bending and steady internal

pressure load. By analysing the result, it was found that shakedown boundaries of miter bends have compact domain sizes as compared to shakedown boundaries of standard round pipe elbow of similar geometrical parameters. It was evident that shakedown boundaries of miter bends increased in size only if number of welds were increased. Hence, miter bend with infinite welded joints could match the shakedown boundaries of smooth pipe bends by amplifying shakedown boundaries. Study also revealed that shakedown domain remained same for both in plane opening and in plane closing bending moments. But study revealed larger shakedown domain when miter bends were tested under out of plane bending load as compared to shakedown domain under in plane bending. Moreover, it was evident that reverse plasticity behaviour was dominating when number of welding joints of miter are reduced as compared to ratcheting response.

Takahashi¹⁷ has conducted experimental investigation on round elbow specimens with local wall thinning subjected to low cycle fatigue. Fatigue life of three elbow specimens were predicted under in plane bending load without internal pressure. Cyclic bending loads were applied to local wall thinned elbow specimen through displacement control. Elastic-Plastic numerical investigations were also carried out to evaluate crack initiation, crack penetration area, crack propagation. Results of finite element analysis justified the evaluated experimental data.

Varelis and Gresnigt¹⁸ investigated fatigue life prediction and allowable local stress amplitude of round elbow under severe cyclic in plane bending both by experimentation and FEA. The FEA results of force-displacement curve and flattening-displacement curves were similar to that of test data recorded. Results were compared with ASME B31.3 and EN 13480-3 standards. Furthermore, by experiment, it has been found that six specimens out of eight specimens failed below 10^5 cycles showing failure due to low cycle fatigue. By testing one specimen it is found that transition from low cycle regime to high cycle regime occurred at 13160 cycles.

Takahashi *et al.*¹⁹ estimated low cycle fatigue life of the elbow specimens made of STPT410 carbon steel subjected to combined cyclic bending and internal pressure, considering the multi-axial stress effect with the help of UTM (Universal testing machine) at room

temperature with pressure limit up to 12 MPa. Local wall thinning effect was observed on behaviour of crack propagation and fatigue life. Conventional and universal slope method was evaluated to investigate effect of ratchet strain on fatigue life, and it was concluded that Manson's universal slope method was substantially nonconservative compared to experimental results as experimental fatigue life were 20% of estimated fatigue lives and so revised Mason's universal slope method was found preferable.

Urabe *et al.*²⁰ investigated low cycle fatigue behaviour of local wall thinned pipe bend specimen. Bend was analysed under seismic load and for both with and without internal pressure. It was reported that fatigue life under low pressure (3MPa) is similar to pipe bend without internal pressure, but as internal pressure increases fatigue life decreases. Furthermore, it was found that though eroded angle and eroded ratio increased up to 180 and 0.5 degrees, respectively, local wall thinned pipe elbows had high margin of safety against seismic loading, compared to ASME Boiler and Pressure Vessel Code Sec. III seismic stress norms. Experiment has also concluded that there is a clear need of fatigue evaluation methodology to evaluate strain behaviour at outer pipe surface of elbow as it is more appropriate and practically required.

Van *et al.*²¹ developed simplified technique to compute the plastic ratchet of pipe elbow subjected to internal pressure and seismic load. Formula was derived to assess the fatigue-ratcheting damage of pipe elbow. Simplified method predicted the magnitude of ratchet without the use of FEA and is accurately applicable to complex plastic response.

Jang *et al.*²² established effective numerical model to evaluate low cycle fatigue behaviour of pipe elbows and approach was validated through cyclic bending test experiment. Following points were concluded after using tie break and erosion numerical models and results were compared with experiment results.

- Tie break method possessed two times quicker computing speed than erosion method to estimate strength of piping system subjected to seismic load.
- Finite element model was easily constructed by using element erosion technique, but recorded

results of crack shape and load-displacement curves were not justifying experimental results.

- Tie break methodology was accurate in representing vibrating load-displacement curves. Tie break method reduced 25% calculation time and fatigue life calculated was closer to experimental data.

Table 3 compiles results of low cycle fatigue test under cyclic in plane bending conducted by some of the above researchers including specimen size, condition of fatigue test, experiment condition, fatigue life crack and location.

Over the years many researchers have developed different mathematical model to estimate fatigue life of elbow bend but many less researches are made on miter bend fatigue life. Table 4 summarises to date fatigue life equations used by various researchers to evaluate fatigue life.

S-N curve approach is widely being used to predict fatigue life of various structural components. Many researchers have used S-N curve approach on pipe welds that are subjected to various loading and joint types. New 2007 ASME Div 2 adopted master S-N curve for fatigue life evaluation of welded components as a substitute of ASME's standard fatigue evaluation process. The master S-N curve (ASME Div 2) was rewritten and validated by Dong and Osage²⁷ using proposed mesh insensitive structural stress method. The master S-N curve has effectively eliminated inclusion of empirical fatigue strength factor by using equivalent structural stress formulation. Study revealed that single S-N master curve could narrow down large weldment S-N data.

Assessment of ASME's Fatigue Strength Reduction Factors (FSRF) for vessels and piping welds was investigated by Dong *et al.*²⁸ using mesh sensitive structural stress method. Proposed method accurately characterised stress concentration and stress intensity at vessel and pipe welds. It was found that a single master S-N curve could be developed irrespective of weld types and geometries by narrowing the data obtained from mesh insensitive structural stress method.

Later, the unified master S-N curve method was developed by Dong and Hong²⁹ for vessel girth and pipe welds using mesh insensitive structural stress method. Based on the investigation it was found that suggested

Table 3. Low cycle fatigue test data.

Author	Condition of Fatigue Test							Results					
	Local Wall Thinning Condition				Experiment Condition			Crack location	Direction of crack	Fatigue life Nf (cycles)			
	Specimen Size (mm)	Material	Location of wall thinning	Eroded Ratio ()	Eroded angle 2 (deg)	Internal Pressure (Mpa)	Disp. (mm)						
Takahashi <i>et al.</i> ¹⁹	Outer Diameter=114.3 Wall Thickness= 6 Radius = 152.4	STPT410 Carbon Steel	Extradados	0.5	180	0	±20	Crown (I.S)	Axial	169			
						3		Crown		173			
						6		Crown		123			
						9		Crown		119			
						12		Crown		103			
						9		Crown		262			
								Crown	15			103	
								Crown	20			50	
								Crown	30			120	
								Crown	-			116	
								Crown	180	9	-		

Varels ²³	Nominal Diameter = 219.1 mm Wall Thickness = 8.18 mm Bend Radius = 305 mm	P355N Alloy Steel	-	0.12	±25	Crown & Weld Region	Axial	13160
					±70	Crown & Weld Region	Axial	444
					±100	Crown & Weld Region	Axial	171
					±150	Crown & Weld Region	Axial	61
					±200	Crown & Weld Region	Axial	28
					±250	Crown & Weld Region	Axial	17
					±300	Crown & Weld Region	Axial	10
					EECS Protocol	Crown & Weld Region	Axial	16
					±200	Crown & Weld Region	Axial	26
					±300	Crown & Weld Region	Axial	10
					±200	Crown & Weld Region	Axial	27
					±300	Crown & Weld Region	Axial	10
					±200	Crown & Weld Region	Axial	22
Jang ²²	Nominal Diameter = 88.9 mm Nominal Thickness = 5.486 mm Bend Radius = 114.3mm	Steel	-	2	±60	Crown	Axial	19.58 (Avg.)
					±80	Crown		11.30 (Avg.)
					±80	Crown		8.44 (Avg.)

Table 4. Fatigue life equations

Author	Structure Type	Loading Condition	Fatigue life equation	Remarks
Tees ²⁴	T-Pipe Bend	IPB	SIF x $s_f = 490000N^{-0.2}$	SIF and fatigue testing of various pipe components
Takahashi <i>et al.</i> ²⁵	90-degree elbow	IPB	$\Delta\varepsilon_t = 0.6158N_f^{-0.0746} + 89.08N_f^{-0.5414}$	Low Cycle Fatigue with local wall thinning
Li <i>et al.</i> ¹⁵	Miter bend	IPB, PRESS	Basquin-Coffin Manson (BCM) equation $\frac{\Delta\varepsilon}{2} = \frac{\sigma_f'}{E} (2N)^b + \varepsilon_f' (2N)^c$ Modified equation $\frac{\Delta\varepsilon}{2} = \frac{(\sigma_f' - \sigma_m)}{E} (2N)^b + (\varepsilon_f' - \varepsilon_r) \left(\frac{(\sigma_f' - \sigma_m)}{\sigma_f'} \right)^{\frac{c}{b}} (2N)^c$	Ratcheting and fatigue behaviour
Takahashi <i>et al.</i> ¹⁷	Elbow	IPB, PRESS	$\Delta\varepsilon = \frac{3.5\sigma_B}{E} N_f^{-0.12} + \varepsilon_f^{0.6} N_f^{-0.6}$	Low cycle fatigue with local wall thinning
Shibutani <i>et al.</i> ²⁶	Elbow	IPB	I. $F = D_f + 2\sqrt{D_f D_d} + D_d$ II. $D_f = \eta^{0.6}$ III. $D_d = \varepsilon_f / \varepsilon_{f0}$ IV. $\varepsilon_{f0} = \ln \frac{100}{100 - \phi}$	Fatigue failure analysis of piping systems with and without thinned elbows on tri-axial shake table tests
Varelis ²³	Elbow	IPB, with and without PRESS	I. $N_f = \left(\frac{8.198}{\Delta\varepsilon} \right)^{3.43}$ II. $K_t^2 = K_\sigma K_\varepsilon$ III. $\Delta\sigma\Delta\varepsilon = K_t^2 \Delta S \Delta\varepsilon$	Local strain and its accumulation at the critical elbow location
Takahashi <i>et al.</i> ¹⁹	Elbow	IPB, PRESS	Manson's Universal Slope Method $\Delta\varepsilon = \frac{3.5\sigma_f}{E} N_f^{-0.12} + \varepsilon_f^{0.6} N_f^{-0.6}$ Revised Manson's Universal Slope Method $\Delta\varepsilon = \frac{3.5\sigma_f}{E} N_f^{-0.12} + \varepsilon_{mf}^{0.6} N_f^{-0.6}$	Low cycle fatigue life considering multiaxial stress effect

Varelis ¹⁸	Elbow	IPB	$I. N_f = \left(\frac{1467.8}{\Delta l}\right)^{2.59}$ $II. N_f = \left(\frac{9.057}{\Delta \varepsilon}\right)^{2.88}$ $III. S_A = (6N_f^{-0.2})[1.25S_h + 0.25S_c]$	Low cycle fatigue under strong cyclic loading
Takahashi <i>et al.</i> ¹⁷	Elbow	PRESS	$I. S_a = K_2 C_2 \frac{M_a}{Z}$ $II. S_a = \frac{1}{2} E \Delta \varepsilon = \frac{3.5\sigma_b}{E} N_f^{-0.12} + \frac{1}{2} E \varepsilon_f^{0.6} N_f^{-0.6}$	Low cycle fatigue behaviour having local wall thinning
Van <i>et al.</i> ²¹	Elbow	PRESS & Seismic loading	$I. \frac{N_{fr}}{N_{fo}} = \left(1 - \frac{r_{max}}{\varepsilon_f}\right)^{-1/c}$ $II. r = \sqrt{2\pi}\sigma^0 A^{max} \beta - \gamma \left(1 - erf\left(\frac{1}{\sqrt{2}\sigma^0 A^{max}}\right)\right)$	Simplified method to calculate the plastic ratchet of elbow-shaped pipes without the use of FEM

approach was accurate to predict fatigue life of welded components.

The master S-N curve method for fatigue evaluation of naval structure was investigated by Dong and Hong³⁰. Curved weld was analysed for structural stress assessment using plate/shell element model. Proposed master S-N curve method simplified fatigue evaluating procedure for ship assemblies and significantly reduced requirements of different tests.

4.3 Creep Fatigue and Vibration Induced Fatigue

Chen *et al.*³¹ investigated effect of temperature on ratcheting behavior of pressurized 90° elbow with internal pressure of 20Mpa and reverse bending of 20kN using experiment method and results were validated FEA results. Ratcheting boundary was determined by Chaboche model combined with C-TFD method. It was concluded that maximum ratcheting strain observed with increase in temperature, moreover maximum ratcheting strain was located at intrados in circumferential direction, moreover, hoop ratcheting strain was larger than that of axial strain.

Shi *et al.*³² developed local collapse solution for elbow end welds to assess defects. Creep fatigue growth was assessed under internal pressure, system moments, high temperature and welding residual stress. An evaluation of creep- fatigue growth was conducted by using R₅ methodology and limiting defect calculation was based on R6-revision 4 procedures. It is observed that final crack depth reached 15.2 mm and weld specimen has completed 88,300 hours before it reached limiting defect depth and so it was concluded that elbow weld can be safe in service for another 88300 hours after the crack initiated.

5.0 Conclusions

Many researchers have conducted numerical analysis and experimental investigation of standard pipe elbow by either considering monotonous load of internal pressure, In Plane Bending (IPB), Out of Plane Bending (OPB) or combine load of mainly cyclic bending and internal pressure. Much less research is made on miter bend subjected to various combine loading though this nonstandard component is still widely used in industries. From literature study following conclusions are stated.

- Theories and mathematical models developed so far have the constraints with varying implication of materials, dimensions, bend type and combination of loading and still FEA is the only method to assess the elastic and plastic behavior of entire range of miter bend. Though various FEA model is improved over the last decade, it still needs development over the entire spectrum of miter bend subjected to combination of loading.
- There is still scope of research in structural assessment of miter bend considering out of circularity, end effects and effects of reinforcement as it is not described thoroughly in standards. There is also scope of creep fatigue of miter bend operated at elevated temperature.
- Vibration induced high cycle fatigue and optimization is not yet attempted so far.

6.0 Acknowledgement

I would like to acknowledge the valuable guidance and support of my colleague Dr. Vratraj Joshi.

7.0 References

1. Green and Emmerson. Stresses in a pipe with a discontinuous bend; 1951.
2. Street S. Multi-mitred and single-mitred bends to internal pressure. *Int J Mech Sci.* 1971; 13:471-88. [https://doi.org/10.1016/0020-7403\(71\)90094-4](https://doi.org/10.1016/0020-7403(71)90094-4)
3. Bond MP. Out-of-plane bending; 1971.
4. Watanabe O, Ohtsubo H. Stress analysis of mitred bends by ring elements. *J Press Vessel Technol.* 1984; 106(1):54-62. <https://doi.org/10.1115/1.3264309>
5. Kitching R, Hose DR. Experimental multi-mitred lined glass reinforced plastic pipe bends. *Int J Mech Sci.* 1995; 37(2):97-119. [https://doi.org/10.1016/0020-7403\(95\)93346-8](https://doi.org/10.1016/0020-7403(95)93346-8)
6. Wood JN. A review of literature for the structural assessment of mitred bends. *Int J Press Vessels Pip.* 2008; 85(5):275-94. <https://doi.org/10.1016/j.ijvpv.2007.11.003>
7. Zhou CY, Leis BN, Feier II. Stress analysis of miter joint in pipeline under internal pressure or in-plane bending loading. *Am Soc Mech Eng Press Vessel Pip Div PVP.* 2010; 6: 1011-19.
8. Chang DS and Redekop D. Stress analysis of pressurized multiple 90 degree mitred pipe bends. 2015. The 4th International Conference on Advances in Structural Engineering and Mechanics (ASEM'08), Jeju Island, South Korea.
9. Orynyak I. The application of long and short cylindrical solutions for stress and flexibility determination in a single mitred bend. *ASME 2016 Pressure Vessels and Piping Conference 2016 Jul 17-21, Vancouver, British Columbia; 2016.*
10. Colquhoun I. Integrity of small angle mitred joints. *IPC2016-64101; 2019.* p. 1-8.
11. Dubyk Y, Seliverstova I, Bogdan A. Stress assessment of single mitred bend using approximate cylindrical shell solutions. *Procedia Struct Integr.* 2019; 18:630-8. <https://doi.org/10.1016/j.prostr.2019.08.209>
12. Neilson R, Wood J, Hamilton R, Li H. A comparison of plastic collapse and limit loads for single mitred pipe bends under in-plane bending. *Int J Press Vessels Pip.* 2010; 87(10):550-8. <https://doi.org/10.1016/j.ijvpv.2010.08.015>
13. Rahman SM, Hassan T, Corona E. Evaluation of cyclic plasticity models in ratcheting simulation of straight pipes under cyclic bending and steady internal pressure. *Int J Plast.* 2008; 24(10):1756-91. <https://doi.org/10.1016/j.ijplas.2008.02.010>
14. Goyal S. Fatigue ratcheting investigation on pressurised elbows made of SS304 LN fatigue ratcheting investigation on pressurised elbows made of SS304 LN. *International Conference on Theoretical, Applied, Computational and Experimental Mechanics, Kharagpur, India; 2010.*
15. Li H, Wood J, McCormack R, Hamilton R. Numerical simulation of ratcheting and fatigue behaviour of mitred pipe bends under in-plane bending and internal pressure. *Int J Press Vessels Pip.* 2012; 101:154-60. <https://doi.org/10.1016/j.ijvpv.2012.11.003>
16. Korba AG, Megahed MM, Abdalla HF, Nassar MM. Shakedown analysis of 90-degree mitred pipe bends. *Eur J Mech A-Solid.* 2013; 40:158-65. <https://doi.org/10.1016/j.euromechsol.2013.01.006>
17. Takahashi K, Watanabe S, Ando K, Urabe Y, Hidaka A, Masakazu Hisatsune, *et al.* Low cycle fatigue behaviors of elbow pipe with local wall thinning. *Nucl Eng Des.* 2009; 239(12):2719-27. <https://doi.org/10.1016/j.nucengdes.2009.09.011>
18. Varelis GE, Karamanos SA, Gresnigt AM. Pipe elbows under strong cyclic loading. *J Press. Vessel Technol.* 2012; 135(1). <https://doi.org/10.1115/1.4007293>

19. Takahashi K, Ando K, Matsuo K, Urabe Y. Estimation of low-cycle fatigue life of elbow pipes considering the multi-axial stress effect. *J Press Vessel Technol.* 2014; 136(4). <https://doi.org/10.1115/1.4026903>
20. Urabe Y, Takahashi K, Sato K, Ando K. Low cycle fatigue behavior and seismic assessment for pipe bend having local wall thinning-influence of internal pressure. *J Press Vessel Technol.* 2013; 135(4). <https://doi.org/10.1115/1.4024444>
21. Van KD, Moumni Z. Evaluation of fatigue-ratcheting damage of a pressurised elbow undergoing damage seismic inputs. *Nucl Eng Des.* 2000; 196(1):41-50. [https://doi.org/10.1016/S0029-5493\(99\)00229-0](https://doi.org/10.1016/S0029-5493(99)00229-0)
22. H. W. Jang, D. Hahm, J. Jung, and J. Hong. *Nucl. Eng. Technol.* 2018.
23. Varelis GE, Karamanos SA. Low-cycle fatigue of pressurized steel elbows under in-plane bending. *J Press Vessel Technol.* 2014; 137(1). <https://doi.org/10.1115/1.4027316>
24. F. Tees. A finite element based study on stress intensification factors (sif) for reinforced. vol. 44. 2011.
25. Takahashi K, Tsunoi S, Hara T, Ueno T, Mikami A, Takada H, *et al.* Experimental study of low-cycle fatigue of pipe elbows with local wall thinning and life estimation using finite element analysis. *Int J Press Vessels Pip.* 2010; 87(5):211-9. <https://doi.org/10.1016/j.ijpvp.2010.03.022>
26. Shibutani T, Nakamura I, Otani A. Failure analysis of piping systems with thinned elbows on tri-axial shake table tests. *J Press Vessel Technol.* 2014; 137(1). <https://doi.org/10.1115/1.4028422>
27. Dong P, Prager M, Osage D. The Design Master S-N Curve in ASME Div 2 rewrite and its validations. *Weld World.* 2007; 51(5-6):53-63. <https://doi.org/10.1007/BF03266573>
28. P. Dong, J. K. Hong, D. Osage, M. Prager, T. Equity, and E. Group. Assessment of asme 's fsrf rules for vessel and piping welds.31-43.
29. Dong P, Hong JK. The Master S-N Curve approach to fatigue of piping and vessel welds. *Weld World.* 2004; 48(1-2):28-36. <https://doi.org/10.1007/BF03266411>
30. P. Dong and J. K. Hong. *OM AE2004-51 324.*2016; 1-9.
31. Chen X, Wang X, Chen X. Effects of temperature on the ratcheting behavior of pressurized 90° elbow pipe under force controlled cyclic loading. *Smart Struct Syst.* 2017; 19(5):473-85. <https://doi.org/10.12989/sss.2017.19.5.473>
32. Shi JH. Creep-fatigue crack growth assessments of elbow end welds. *Procedia Eng.* 2015; 130:893-901. <https://doi.org/10.1016/j.proeng.2015.12.218>

Nomenclature

Z	Section modulus
E	Young's Modulus
s_f	Stress range to failure
H	Flexibility characteristic
M_{FY}	First yield moment
M_L	Collapse Moment
M_{GY}	Gross yield moment
F_{GY}	Gross Yield Load
F_L	Collapse Load
P_{GY}	Gross Yield Pressure
P_L	Burst/Collapse Pressure
P_{FY}	First Yield Pressure
σ^0	Standard Deviation
r_{max}	Ratchet (Simplified technique)
ϵ_f	Material Ductility
c	Material Constant
erf	Error function
r	Ratchet
F	Fatigue factor

D_f	Fatigue damage
D_d	Ductility consumption
$\Delta\sigma$	Local peak stress range
ϕ	Reduction in area
σ_f'	Fatigue strength coefficient
ε_f'	Fatigue ductility coefficient
σ_m	Mean stress
ε_r	Ratchet strain
N	Number of cycles
b	Fatigue strength exponent
c	Fatigue ductility exponent
$\Delta\varepsilon$	Strain Range/ Hoop Strain Range
σ_B	Tensile Strength
ΔS	Nominal stress range
$\Delta\varepsilon_t$	Applied total strain range
σ_f	True fracture strength
ε_{mf}	Multi-axial fracture ductility
Δl	End Displacement Amplitude
S_A	Allowable local stress amplitude
S_a	Fictitious stress amplitude
K_2	Peak stress index for bending load
C_2	Secondary stress indices
M_a	Fictitious moment amplitude
S_h	Allowable stresses at largest temperature of metal
S_c	Allowable stresses at least temperature of metal
N_f	Fatigue Life/Number of cycles to failure
K_σ	Stress concentration factor (Plastic)
K_ε	Strain concentration factor (Plastic)
K_t	Elastic stress concentration factor (Theoretical)
N_{fr}	Number of cycles to failure (combination of cyclic strain and ratchet)
N_{f_0}	Number of cycles to failure (cyclic strain only)
β	Slopes of the plastic parts of the curve for closing
γ	Slopes of the plastic parts of the curve for opening
A^{max}	Maximum value of the imposed rotation
ε_{f_0}	True rupture ductility/ fracture strain
ε_f	Accumulated strain/ Full fracture ductility

Acronyms

IPB	In Plane Bending
OPB	Out of Plane Bending
TORS	Torsions
PRESS	Pressure
SIF	Stress intensification factor